Journal of Alloys and Compounds 559 (2013) 146–151

Contents lists available at SciVerse ScienceDirect

Journal of Alloys and Compounds

journal homepage: www.elsevier.com/locate/jalcom

Fabrication of hafnia hollow nanofibers by atomic layer deposition using electrospun nanofiber templates

Inci Donmez, Fatma Kayaci, Cagla Ozgit-Akgun, Tamer Uyar *, Necmi Biyikli *

UNAM – Institute of Materials Science and Nanotechnology, Bilkent University, Ankara 06800, Turkey

ARTICLE INFO

Article history:
Received 7 November 2012
Received in revised form 4 January 2013
Accepted 11 January 2013
Available online 4 February 2013

Keywords:
Atomic layer deposition
Electrospinning
HfO_2
Hollow nanofibers
Nylon 6,6

ABSTRACT

Hafnia (HfO_2) hollow nanofibers (HNs) were synthesized by atomic layer deposition (ALD) using electrospun nylon 6,6 nanofibers as templates. HfO_2 layers were deposited on polymeric nanofibers at 200 °C by alternating reactant exposures of tetrakis(dimethylamido)hafnium and water. Polymeric nanofiber templates were subsequently removed by an *ex situ* calcination process at 500 °C under air ambient. Morphological and structural characterizations of the HN samples were conducted by scanning electron microscopy, transmission electron microscopy and X-ray diffraction. Freestanding network of HfO_2 HNs was found to be polycrystalline with a monoclinic crystal structure. Elemental composition and chemical bonding states of the resulting HfO_2 HNs were studied by using X-ray photoelectron spectroscopy. The presence of HfO_2 was evidenced by high resolution scans of Hf 4f and O 1s with binding energies of 16.3–17.9 and 529.6 eV, respectively. Combination of electrospinning and ALD processes provided an opportunity to precisely control both diameter and wall thickness of the synthesized HfO_2 HNs.

1. Introduction

Atomic layer deposition (ALD) is a thin film deposition technique based on saturative surface reactions. Despite being a chemical vapor deposition method, the distinctive feature of ALD is that each exposure of a single precursor is followed by purging/evacuation of the growth chamber. Since the precursors are exposed one at a time, the gas–solid reactions occurring at the surface terminate after all available reaction sites are covered. This self-limiting film growth mechanism results in a number of attractive features, such as precise film thickness control and ultimate conformality, uniformity over large sample sizes, and high quality films deposited at relatively low temperatures [1]. Combination of these properties inspired ALD to be used in many technological applications including gate dielectric and diffusion barrier layers in CMOS integrated circuits, humidity barriers, anti-reflective coatings and encapsulation layers for solar cells, transparent conducting films for transparent electronics, anti-stiction layers in micro-electromechanical devices, encapsulation and active films for three-dimensional solid-state batteries, catalyzer coatings for membranes, and bio-compatible coatings for medical implants [2,3].

Besides conventional thin film deposition on planar surfaces and substrates, ALD has also been effectively used for synthesizing various nanostructures such as nanoparticles, nanotubes, and nanobelts, through template-based routes. Due to its conformal deposition capability at low temperatures, a wide selection of materials has been used as nanostructured templates for ALD growth. Among these, anodic aluminum oxide (AAO) is the most widely reported template, which was in general used for the synthesis of oxide nanotubes by ALD [4–8]. Elemental/compound semiconductor and carbon nanotube templates have been used as well for synthesizing hollow nanostructures [9,10]. Several groups have used electrospun polymeric nanofibers as templates to synthesize nanotubes of Al_2O_3 [11,12], SnO_2 [13], TiO_2 [14–16], and ZnO [11,17–19] using ALD. In these studies, electrospun nanofibers of poly(vinyl alcohol) [11,12], polyacrylonitrile [13], poly(vinyl pyrrolidone) [14,15], and poly(vinyl acetate) [16–19] were used as polymeric nanofiber templates. Recently, we have used electrospun nylon 6,6 nanofibers for synthesizing hollow AlN [20] and core–shell nylon 6,6-ZnO [21] nanofibers.

Nanotubes of oxide materials exhibit attractive electrical properties and thus have potential applications in microelectronics. Among these materials, hafnia (HfO_2) has attracted significant interest due to its high thermal and mechanical stability, chemical inertness, rather large band gap (~5.8 eV), high dielectric constant and refractive index, as well as good transparency in the visible spectral range and low phonon energies [22,23]. Several different templates were reported to be used in the synthesis of HfO_2 nanotubes via ALD. Hafnia nanotubes obtained by using AAO templates were studied by several groups [24–26]. Similar structures were synthesized by depositing a conformal HfO_2 layer on porous silicon templates [27]. In 2009, Shandalov and McIntyre studied the size

* Corresponding authors. Tel.: +90 312 290 3556.
E-mail addresses: tamer@unam.bilkent.edu.tr (T. Uyar), biyikli@unam.bilkent.edu.tr (N. Biyikli).

0925-8388/$ - see front matter © 2013 Elsevier B.V. All rights reserved.
http://dx.doi.org/10.1016/j.jallcom.2013.01.064

dependent polymorphism of HfO_2 nanotubes synthesized by using Ge (1 1 1) nanowire arrays as templates [28]. Recently, carbon nanotubes were coated with HfO_2 using ALD in order to study the field emission properties of the designed structure [29]. However, to the best of our knowledge, synthesis of HfO_2 hollow nanofibers by combining electrospinning and ALD has not yet been reported.

In this study, gaseous precursors of tetrakis(dimethylamido) hafnium ($Hf(NMe_2)_4$) and water (H_2O) have been used for the deposition of HfO_2 films over electrospun nylon 6,6 nanofiber templates having average fiber diameters of 70 and 330 nm. After the removal of polymeric templates by calcination, HfO_2 hollow nanofibers (HNs) were obtained with controlled inner diameter, wall thickness and crystallinity. Here we report on the morphological, structural and compositional characterization of HfO_2 HNs synthesized by ALD using electrospun nanofiber templates.

2. Experimental procedure

Nylon 6,6 nanofibers having different average fiber diameters were obtained by electrospinning. Polymer solutions were prepared by dissolving 5% (w/v) nylon 6,6 in 1,1,1,3,3,3-hexafluoro-2-propanol (HFIP) (Sigma–Aldrich, ⩾99%) and 8% (w/v) nylon 6,6 in formic acid (Sigma–Aldrich, 98–100%). Prepared solutions were stirred for 3 h at room temperature. Viscosities of the nylon 6,6 solutions were measured by using Anton Paar Physica MCR-301 Rheometer equipped with cone/plate accessory using the spindle type CP40-2 at 22 °C and a constant shear rate of 100 s^{-1}. Homogeneous nylon 6,6 solutions were then placed in 3 ml syringes fitted with metallic needles of 0.8 mm inner diameter. Syringes were fixed horizontally on the syringe pump (Model: SP 101IZ, WPI). Polymer solutions were pumped with a feed rate of 1 ml/h during electrospinning. 15 kV was applied to the metal needle tip by using a high voltage power supply (Matsusada, AU Series). Tip-to-collector distance was set at 10 cm. On the way to the grounded stationary cylindrical metal collector (height: 15 cm, diameter: 9 cm), solvents evaporated and nylon 6,6 nanofibers were deposited on an aluminum foil covering the collector. Electrospinning processes were carried out at 23 °C and 36% relative humidity in an enclosed Plexiglas box. Fig. 1a shows the schematic representation of electrospinning process.

Following the fabrication of nylon 6,6 nanofibers by electrospinning, these polymeric templates were introduced into the ALD system (Savannah S100 ALD reactor, Cambridge Nanotech Inc.) and coated with HfO_2. Depositions were performed at 200 °C using $Hf(NMe_2)_4$ and H_2O as the organometallic precursor and oxygen source, respectively (Fig. 1b). $Hf(NMe_2)_4$ was preheated to 75 °C and stabilized at this temperature prior to depositions. N_2 was used as the carrier gas with a flow rate of 20 sccm. Pulse times of the Hf precursor and oxygen source were 0.2 and 0.015 s, which were followed by 15 and 10 s purge periods, respectively. Two deposition modes were used: (1) with continuous pumping (base pressure = 0.25 Torr) (i.e. deposition mode 1), and (2) with pump valve closed during the pulse steps and opened during the purge steps of the ALD cycle (i.e. deposition mode 2). Using deposition mode 1,200 cycles HfO_2 was deposited on a solvent-cleaned planar Si (1 0 0) substrate at 200 °C. Thickness of the HfO_2 layer was measured by spectroscopic ellipsometry as 22 nm, corresponding to a deposition rate of 1.1 Å/cycle. Regardless of the deposition mode, 600 ALD cycles were applied. After the depositions, calcination process was performed at 500 °C for 2 h under atmospheric conditions in order to remove the core polymeric nanofibers (Fig. 1c).

Nova NanoSEM scanning electron microscope (FEI) was used to reveal morphology, uniformity and dimensions of the samples coated with ~5 nm Au/Pd. Average fiber diameters of the electrospun nylon 6,6 nanofibers were calculated by measuring diameters of ~100 fibers from scanning electron microscopy (SEM) images. Chemical composition and bonding states of the synthesized HfO_2 HNs were determined by X-ray photoelectron spectroscopy (XPS), using a Thermo Scientific K-Alpha spectrometer equipped with a monochromatic Al Kα X-ray source. X-ray diffraction (XRD) measurements were performed in a PANalytical X'Pert PRO Multi-Purpose X-Ray Diffractometer operating at 45 kV and 40 mA, using Cu Kα radiation (λ = 0.15418 nm). Transmission electron microscopy (TEM) imaging and selected area electron diffraction (SAED) studies were performed by using a Tecnai G2 F30 transmission electron microscope (FEI). TEM samples were prepared by dispersing the HNs in ethanol by sonification, drop-casting the solution onto a Cu grid, and drying it.

3. Results and discussion

In order to obtain HfO_2 HNs having different inner diameters, nylon 6,6 nanofibers having different average fiber diameters were obtained by the electrospinning technique and these polymeric nanofibers were then used as templates. In electrospinning, fiber diameters strongly depend on the viscosity of polymer solution, therefore, solvent type used and concentration of the polymer solution are important parameters to control the diameter of electrospun fibers [30,31]. Uniform and bead-free nylon 6,6 nanofibers having average fiber diameters of 70 and 330 nm were achieved by

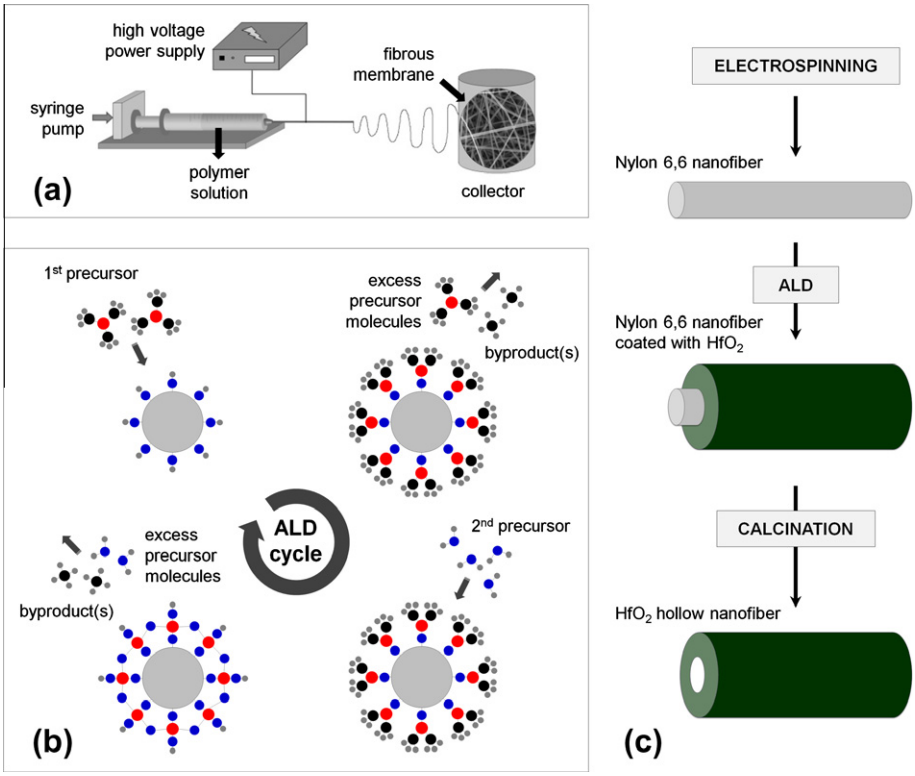

Fig. 1. Schematic representations of (a) electrospinning, and (b) ALD processes. (c) Schematics of the process used to fabricate HfO_2 HNs.

using different solvent systems and polymer concentrations with the viscosities of 0.0228 and 0.115 Pa s, respectively. Fig. 2a shows the representative SEM image of nylon 6,6 nanofibers obtained by electrospinning of the solution prepared by dissolving 5% (w/v) nylon 6,6 in HFIP. Similarly, Fig. 2b is the representative SEM image of nanofibers obtained by the electrospinning of 8% (w/v) nylon 6,6 solution prepared with formic acid solvent system. Nylon 6,6 nanofibers with a much thinner average fiber diameter (70 ± 30 nm) were obtained from formic acid solvent system whereas thicker fibers (330 ± 80 nm) were obtained from HFIP solvent system. This is due to the higher viscosity of polymer solution in HFIP since less stretching of the electrified jet was occurred for more viscous polymer solution during the electrospinning process and therefore larger fiber diameters were obtained [30].

In this study, electrospun nylon 6,6 nanofibers having average fiber diameters of 330 and 70 nm were used as templates for the fabrication of HfO_2 HNs (Fig. 2a and b). Following the deposition of HfO_2 on electrospun nanofiber templates by ALD, coated samples were calcined in order to obtain HfO_2 HNs. Representative SEM images of the nylon 6,6 nanofiber templates having average fiber diameters of 330 and 70 nm after the deposition of 600 cycles HfO_2 at 200 °C are given in Fig. 2c and d, respectively. As clearly seen from these SEM images, a uniform and conformal HfO_2 layer was deposited on electrospun nanofibers using the self-limiting nature of the ALD process. Desired wall thickness was achieved by adjusting the number of deposited ALD cycles. Fig. 2e and f show the resulting HfO_2 HNs obtained by the calcination of HfO_2-coated nylon 6,6 nanofiber templates. For both templates,

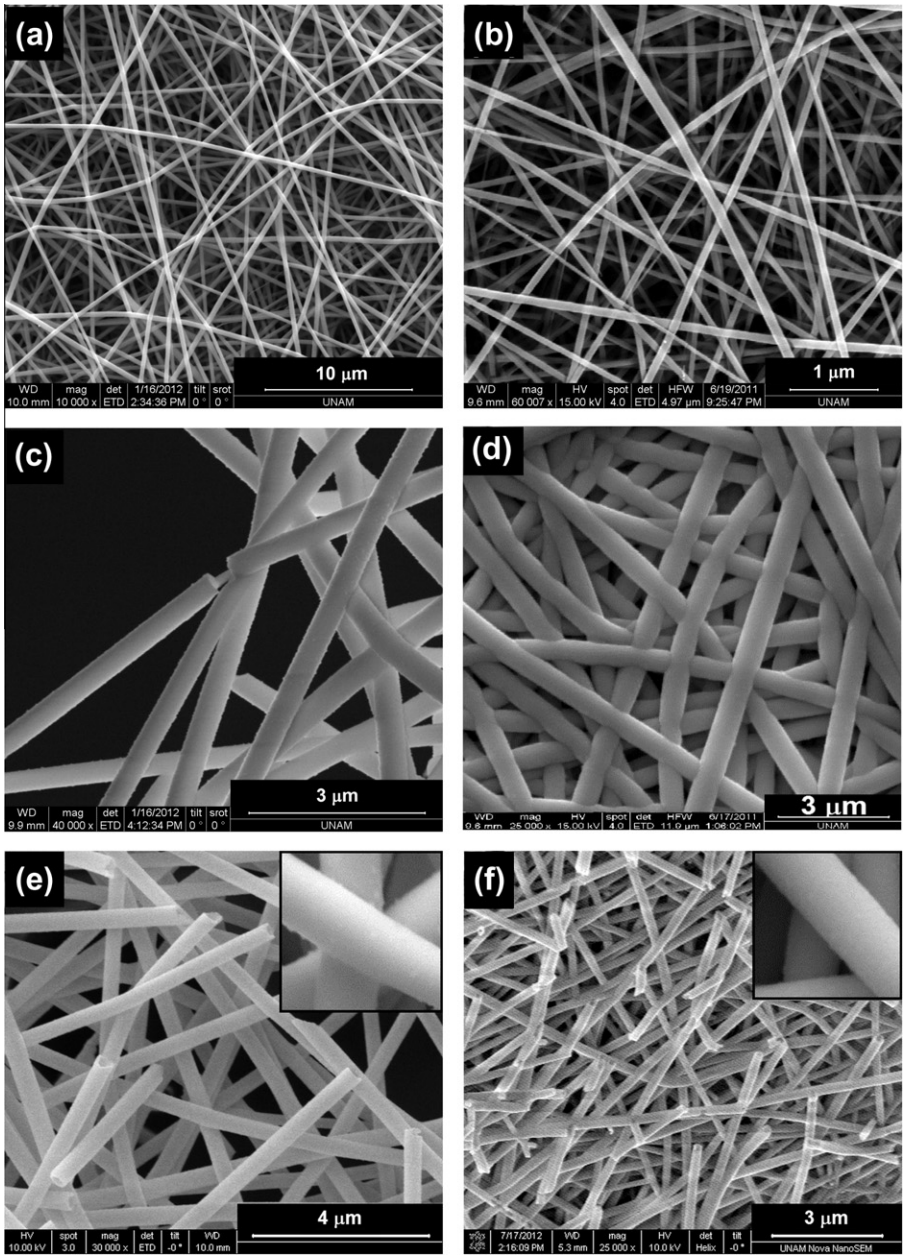

Fig. 2. Representative SEM images of (a and b) electrospun nylon 6,6 nanofibers having ~330 and ~70 nm fiber diameters, respectively, (c and d) same electrospun nanofibers coated with 600 cycles HfO_2 at 200 °C, and (e and f) HfO_2 HNs obtained by calcination. Insets are the magnified SEM images revealing the surface morphologies of calcined samples.

integrity of the structure was well preserved after the calcination step and a freestanding HfO_2 HN network with a uniform and smooth structure was obtained. Flexibility of the samples, however, was lost after the calcination treatment due to the missing polymeric core nanofibers. Samples became brittle and vulnerable to mechanical impacts which may arise during handling. As a result, calcined samples appeared as broken hollow nanofibers in their representative SEM images. Magnified SEM images of HfO_2 HNs prepared with electrospun nylon 6,6 nanofiber templates having average fiber diameters of 330 and 70 nm are given in the insets of Fig. 2e and f, respectively. Surfaces of the synthesized nanostructures were found to be extremely smooth. Small particle-like structures on the surfaces of individual HNs are due to the ~5 nm Au/Pd alloy deposited on samples prior to SEM imaging.

Detailed morphology of the samples was studied by TEM, which confirmed the uniform and conformal structure of synthesized HfO_2 HNs. Fig. 3a shows the TEM image of an individual HfO_2 HN synthesized by depositing 600 cycles HfO_2 on electrospun nanofibers with 330 nm average fiber diameter, followed by a heat treatment carried out under air ambient at 500 °C for 2 h. Wall thickness was measured as ~65 nm from this image, which is quite consistent with the 1.1 Å/cycle deposition rate of HfO_2 ALD at 200 °C. When the very identical ALD growth parameters were applied to electrospun nylon 6,6 nanofiber templates having 70 nm average fiber diameter, the deposition resulted in a ~15 nm wall thickness (Fig. 3b). This might be due to the limited exposure time of the partial pressure above the template to reach full saturation, or limited time for diffusion. This claim was tested by performing the same HfO_2 deposition (600 cycles at 200 °C with the same pulse and purge times) using deposition mode 2 on a template having 70 nm average fiber diameter. In this deposition mode, dynamic vacuum is switched to static vacuum just before the precursor pulses, and switched back to dynamic vacuum before the purging periods after waiting for some time and allowing precursor molecules to diffuse into the high-density and high-surface area electrospun nanofiber template. This process resulted in ~65 nm wall thickness as shown in Fig. 3c, which supported our postulation. This result indicated that the ALD deposition mode should be carefully optimized when growth is going to be carried out on high-surface area substrates.

Chemical compositions and bonding states of the synthesized HfO_2 HNs were studied by using XPS. Survey scan detected 25.6 at.% Hf, 58.4 at.% O, and 16.0 at.% C for the HfO_2 HNs prepared by using a template having 330 nm average fiber diameter. Elemental composition of the HfO_2 HNs prepared by using a template having 70 nm average fiber diameter was found as 25.1 at.% Hf, 56.7 at.% O, and 18.2 at.% C. Fig. 4a and b are the Hf 4f and O 1s high resolution XPS scans obtained from HfO_2 HNs with ~330 nm inner diameter, which were fitted by using subpeaks in order to reveal the bonding states exist in the material. Hf $4f_{7/2}$ and Hf $4f_{5/2}$ subpeaks of the Hf 4f doublet located at 16.3 and 17.9 eV, respectively, were found to be related to the Hf–O bonding in HfO_2 [32]. O 1s scan (Fig. 4b) was fitted by using two subpeaks located at 529.6 and 531.2 eV, revealing the O–Hf and O–H bonds, respectively [33]. The O–Hf/O–H subpeak ratio (i.e. the ratio of integrated intensities) was found as 5.88, indicating that 85.5% of the O detected in this sample is associated with the formation of HfO_2, corresponding to 49.9 at.% O in the sample. By using this information, Hf:O ratio was calculated as 0.51, and it was concluded that the deposited HfO_2 is almost stoichiometric. 16 at.% C found in the sample, on the

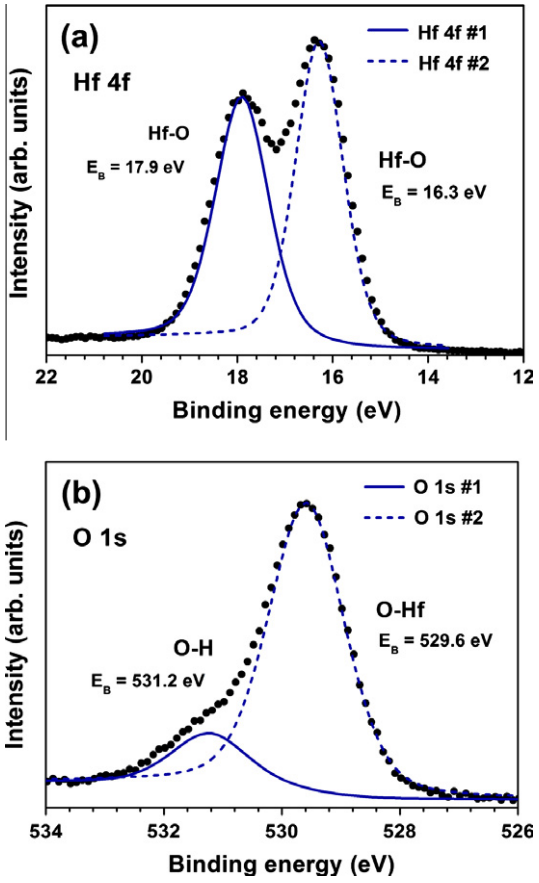

Fig. 4. (a) Hf 4f doublet, and (b) O 1s high resolution XPS scans of the HfO_2 HNs prepared by using a nanofiber tamplate having ~330 nm fiber diameter.

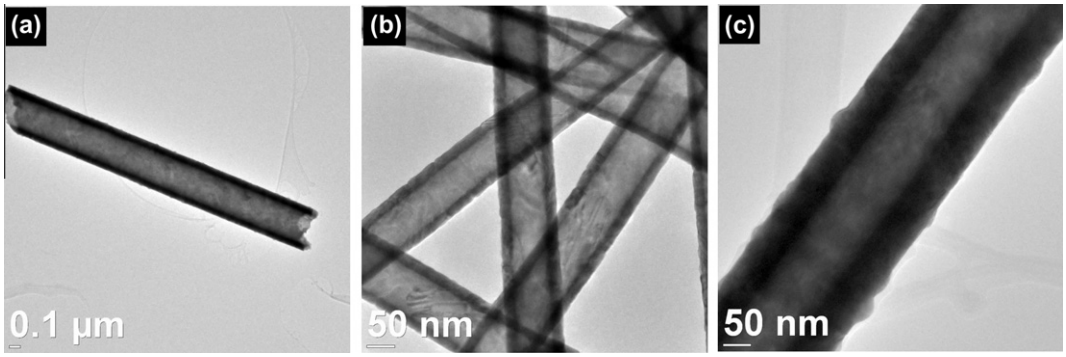

Fig. 3. Representative TEM images of (a) an individual HfO_2 HN with an inner diameter of ~300 nm and a wall thickness of ~65 nm deposited by mode 1, (b) HfO_2 HNs with an inner fiber diameter of ~70 nm and a wall thickness of ~15 nm deposited by mode 1, and (c) HfO_2 HNs with an inner fiber diameter of ~70 nm and a wall thickness of ~65 nm deposited by mode 2.

other hand, was neither bonded to Hf or O, therefore suggested surface contamination. Hf 4f and O 1s high resolution XPS scans obtained from HfO_2 HNs prepared by using a nanofiber template with 70 nm average fiber diameter exhibited the same bonding states. The O–Hf/O–H subpeak ratio was found as 5.56, indicating that 84.8% of the total O is associated with the formation of HfO_2, corresponding to 48 at.% O in sample. Hf:O ratio was calculated as 0.52, again indicating nearly stoichiometric HfO_2.

Fig. 5 shows the XRD patterns of electrospun nylon 6,6 nanofiber template with 330 nm average fiber diameter, template coated with 600 cycles HfO_2, and HfO_2 HNs synthesized by the calcination of coated template at 500 °C for 2 h under air ambient. Similar patterns were obtained for the samples prepared by using a nanofiber template having 70 nm average fiber diameter. Electrospun nylon 6,6 nanofiber template has two characteristic peaks at 20.45° and 23.27° as determined from the XRD patterns of pristine nylon 6,6 nanofibers. After the deposition of 600 cycles HfO_2, characteristic XRD peaks of the nylon 6,6 nanofiber template disappeared. As-deposited HfO_2 layer was nanocrystalline as determined from the XRD pattern obtained from coated nylon 6,6 nanofibers. Upon calcination at 500 °C for 2 h under air ambient, HfO_2 layer became crystalline with a monoclinic structure, which is thermodynamically the most stable polymorph of hafnia [34]. This transition was in agreement with the literature reported for HfO_2 thin films annealed at 500 °C [35].

Fig. 6 reveals the high resolution TEM (HR-TEM) image and SAED pattern of HfO_2 HNs synthesized by depositing 600 cycles HfO_2 on electrospun nanofibers having average fiber diameter of 330 nm, followed by calcination under air ambient at 500 °C for 2 h. HR-TEM image of the sample (Fig. 6a) indicated a polycrystalline structure, which is in good agreement with the XRD results. SAED pattern of the HfO_2 HNs (Fig. 6b) consisted of a series of diffraction rings, further revealing the polycrystalline nature of the HN sample. Bright spots seen on these polycrystalline diffraction rings are indicators of large crystallite size.

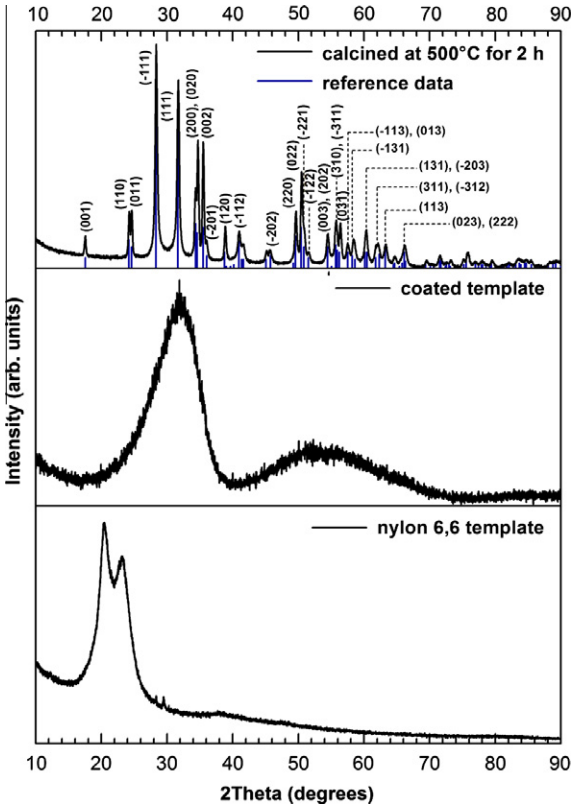

Fig. 5. XRD patterns of electrospun nylon 6,6 nanofibers with ~330 nm fiber diameter, nanofiber templates coated with 600 cycles HfO_2 at 200 °C using ALD, and the resulting HfO_2 HNs after the calcination of coated templates at 500 °C under atmospheric ambient. Reference data for the monoclinic HfO_2 phase is also included (ICDD reference code: 00-034-0104).

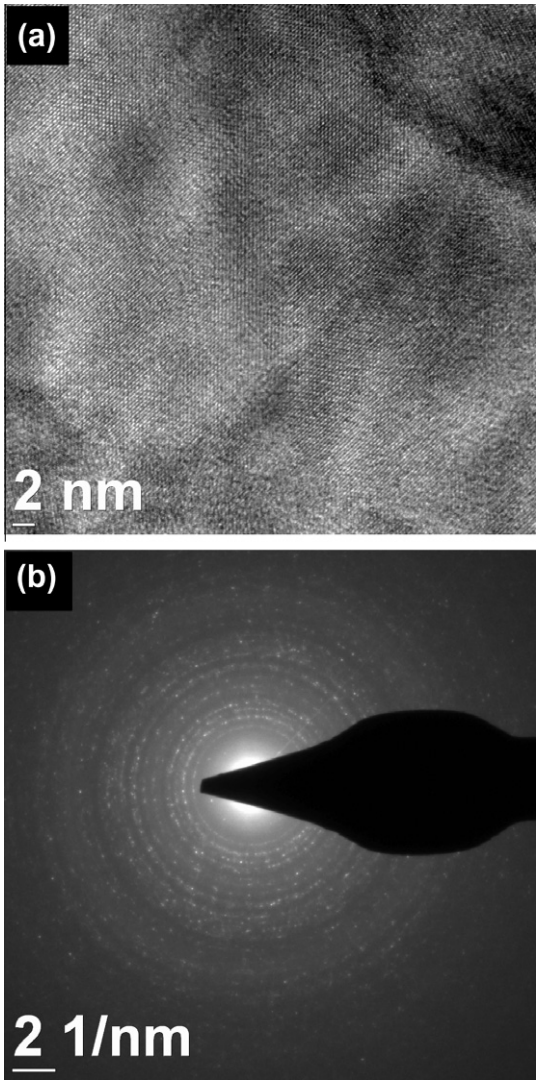

Fig. 6. (a) HR-TEM image of an individual HfO_2 HN with ~330 nm inner diameter and ~65 nm wall thickness. (b) SAED pattern of the synthesized HfO_2 HNs.

4. Conclusions

In this study, we have reported on the template-based synthesis and characterization of HfO_2 HNs. Inorganic HNs were synthesized by depositing HfO_2 on electrospun nylon 6,6 nanofiber templates by ALD, which was followed by the removal of polymeric template by calcination. SEM and TEM studies have shown that the HfO_2 layer deposited by ALD adapted the shape and dimensions of electrospun nanofibers easily as a result of the self-terminating gas–solid reactions occurring at sample surface. After calcining the HfO_2-coated samples at 500 °C under atmospheric conditions, freestanding HN networks were obtained, sustaining the entire template thickness. Formation of stoichiometric HfO_2 was evidenced by XPS measurements. Synthesized HfO_2 HNs were found to be polycrystalline with a monoclinic structure by means of

XRD. While the inner diameter of HfO_2 HNs can easily be varied by using nanofiber templates with different average fiber diameters, which can be achieved by controlling the parameters used in electrospinning process, the wall thickness with sub-nanometer accuracy can be readily controlled by the ALD process. When ALD deposition procedure was applied with continuous pumping on nanofibers with different diameters, thinner wall thicknesses were obtained for the nanofibers having smaller diameters due to either limited exposure time of the partial pressure above the template to saturate its large surface area, or limited time for diffusion. Thus, ALD deposition was carried out with pump valve closed during the pulse steps and opened during the purge steps of the ALD cycle in order to obtain desired thickness while coating high surface area nanofibers. In short, it has been shown that combining electrospinning and ALD methods enables the synthesis of inorganic HNs with precisely controlled dimensions.

Acknowledgements

This work was performed at UNAM supported by the State Planning Organization (DPT) of Turkey through the National Nanotechnology Research Center Project. Authors acknowledge M. Guler from UNAM for TEM measurements. T. Uyar and N. Biyikli acknowledge Marie Curie International Reintegration Grant (IRG) for funding NANOWEB (PIRG06-GA-2009-256428) and NEMSmart (PIRG05-GA-2009-249196) projects, respectively. F. Kayaci and C. Ozgit-Akgun acknowledge TUBITAK-BIDEB for National PhD Scholarship.

References

[1] M. Leskela, M. Ritala, Thin Solid Films 409 (2002) 138–146.
[2] H. Kim, H.-B.-R. Lee, Q.-J. Maeng, Thin Solid Films 517 (2009) 2563–2580.
[3] E. Marin, A. Lanzutti, F. Andreatta, et al., Corros. Rev. 29 (2011) 191–208.
[4] Y.-S. Min, Y.J. Cho, J.-H. Ku, et al., J. Electrochem. Soc. 152 (2005) F124–F128.
[5] A.B.F. Martinson, J.W. Elam, J.T. Hupp, et al., Nano Lett. 7 (2007) 2183–2187.
[6] Y.-H. Chang, S.-M. Wang, C.-M. Liu, et al., J. Electrochem. Soc. 157 (2010) K236–K241.
[7] J. Lee, H. Ju, J.K. Lee, et al., Electrochem. Commun. 12 (2010) 210–212.
[8] Y. Qin, A. Pan, L. Liu, et al., ACS Nano 5 (2011) 788–794.
[9] J. Hwang, B. Min, J.S. Lee, et al., Adv. Mater. 16 (2004) 422–425.
[10] J.S. Lee, B. Min, K. Cho, et al., J. Cryst. Growth 254 (2003) 443–448.
[11] Q. Peng, X.-Y. Sun, J.C. Spagnola, et al., ACS Nano 3 (2009) 546–554.
[12] P. Heikkilä, T. Hirvikorpi, H. Hilden, et al., J. Mater. Sci. 47 (2012) 3607–3612.
[13] B.-S. Lee, W.-S. Kim, D.-H. Kim, et al., Smart Mater. Struct. 20 (2011) 105019.
[14] G.-M. Kim, S.-M. Lee, G.H. Michler, et al., Chem. Mater. 20 (2008) 3085–3091.
[15] E. Santala, M. Kemell, M. Leskela, et al., Nanotechnology 20 (2009) 035602–035606.
[16] S.-W. Choi, J.Y. Park, C. Lee, et al., J. Am. Ceram. Soc. 94 (2011) 1974–1977.
[17] J.Y. Park, S.-W. Choi, J.-W. Lee, et al., J. Am. Ceram. Soc. 92 (2009) 2551–2554.
[18] S.-W. Choi, J.Y. Park, S.S. Kim, Nanotechnology 20 (2009) 465603–465608.
[19] J.Y. Park, S.-W. Choi, S.S. Kim, Nanotechnology 21 (2010) 475601–475609.
[20] C. Ozgit-Akgun, F. Kayaci, I. Donmez, et al., J. Am. Ceram. Soc., article in press, doi: 10.1111/jace.12030.
[21] F. Kayaci, C. Ozgit-Akgun, I. Donmez, et al., ACS Appl. Mater. Interfaces 4 (2012) 6185–6194.
[22] L.X. Liu, Z.W. Ma, Y.Z. Xie, et al., J. Appl. Phys. 107 (2010) 024309.
[23] X. Qiu, J.Y. Howe, M.B. Cardoso, et al., Nanotechnology 20 (2009) 455601–455609.
[24] P. Banerjee, W.-A. Chiou, G.W. Rubloff, Microsc. Microanal. 15 (2009) 1250–1252.
[25] D. Gu, H. Baumgart, G. Namkoong, et al., Electrochem. Solid St. 12 (2009) K25–K28.
[26] I. Perez, E. Robertson, P. Banerjee, et al., Small 4 (2008) 1223–1232.
[27] T.M. Abdel-Fattah, D. Gu, H. Baumgart, ECS Trans. 41 (2011) 139–144.
[28] M. Shandalov, P.C. McIntyre, J. Appl. Phys. 106 (2009) 084322.
[29] Y. Il Song, C.-M. Yang, L.K. Kwac, Appl. Phys. Lett. 99 (2011) 153115.
[30] S. Ramakrishna, K. Fujihara, W. Teo, World Scientific Publishing Company, 2005.
[31] T. Uyar, F. Besenbacher, Polymer 49 (2008) 5336–5343.
[32] M.-H. Cho, Y.S. Roh, C.N. Whang, et al., Appl. Phys. Lett. 81 (2002) 472–474.
[33] D.-P. Kim, G.-H. Kim, J.-C. Woo, et al., J. Korean Phys. Soc. 54 (2009) 934–938.
[34] G. Štefanić, S. Musić, K. Molčanov, J. Alloys Comp. 387 (2005) 300–307.
[35] Y.-K. Chiou, C.-H. Chang, T.-B. Wu, J. Mater. Res. 22 (2007) 1899–1906.